Research Square

Preprints are preliminary reports that have not undergone peer review.
They should not be considered conclusive, used to inform clinical practice,
or referenced by the media as validated information.

A Probiotic-Derived Oxydifficidin from Bacillus subtilis Y4 Combines Direct Antibacterial Activity and Immunomodulatory Effects Against Multidrug-Resistant Acinetobacter baumannii Infection

Xinyuan Li
Jilin Agricultural University
Haowen Yan
Jilin Agricultural University
Jinyu Mou
Jilin Agricultural University
JinYang Gu
Jilin Agricultural University
Lili Guan
Jilin Agricultural University
Jingrui Chen
Jilin Agricultural University
Lingcong Kong
Jilin Agricultural University
Hongxia Ma
Jilin Agricultural University
Haipeng Zhang
zhanghaipeng211@163.com

Jilin Agricultural University

Research Article

Keywords: Antimicrobial compound, Bacillus subtilis, Membrane disruption, Acinetobacter baumannii, Transcriptomic analysis

Posted Date: July 3rd, 2026

DOI: https://doi.org/10.21203/rs.3.rs-10138552/v1

License: This work is licensed under a Creative Commons Attribution 4.0 International License.
Read Full License

Additional Declarations: No competing interests reported.

Abstract

Multidrug-resistant *Acinetobacter baumannii* is a major opportunistic pathogen responsible for severe nosocomial infections, particularly pneumonia in immunocompromised patients. The development of novel antimicrobial agents from beneficial microorganisms represents a promising strategy to combat resistant pathogens. In this study, we investigated the antibacterial activity, active metabolites, antimicrobial mechanisms, and therapeutic potential of *Bacillus subtilis* Y4 isolated from Changbai Mountain soil.

The n-butanol extract of *B. subtilis* Y4 fermentation broth exhibited broad-spectrum antibacterial activity against nine pathogenic bacteria, with minimum inhibitory concentration (MIC) ranging from 16 to 256 μg/mL. Notably, the extract showed potent activity against multidrug-resistant *A. baumannii* with an MIC of 16 μg/mL. Bioassay-guided purification and high-resolution mass spectrometry identified oxydifficidin, a difficidin-family polyketide derivative with a molecular weight of 559.28925 Da. Oxydifficidin exhibited favorable stability and biosafety characteristics, including low hemolytic activity and no detectable acute toxicity.

Mechanistic studies demonstrated that oxydifficidin exerted antibacterial effects by disrupting bacterial membrane integrity, increasing membrane permeability, inducing intracellular reactive oxygen species accumulation, dissipating membrane potential, inhibiting biofilm formation, and promoting leakage of intracellular components. In an immunosuppressed mouse model of *A. baumannii*-induced acute pneumonia, oxydifficidin significantly reduced pulmonary bacterial burden, alleviated lung tissue damage, and suppressed the expression of inflammatory cytokines, including IL-6, TNF-α, and IL-1β. Transcriptomic analysis revealed that oxydifficidin regulated immune-related pathways, particularly cytokine–cytokine receptor interaction and retinol metabolism.

Collectively, this study identifies oxydifficidin as a promising antimicrobial metabolite derived from *B. subtilis* Y4 and highlights its potential application against multidrug-resistant bacterial infections.

1. Introduction

Acinetobacter baumannii will develops high resistance to a variety of commonly used antibiotics, including carbapenems, which makes treatment extremely difficult [1]. Among them, the widespread spread of drug-resistant strains, such as multidrug-resistant *Acinetobacter baumannii* and pandrug-resistant *Acinetobacter baumannii*, further exacerbates the complexity of treatment and is one of the leading causes of nosocomial infections in the current healthcare system [2] In the intensive care unit, *Acinetobacter baumannii* infection has a high incidence of pneumonia, which is difficult to treat and has a high case fatality rate. In the "2024 List of Key Bacterial Pathogens" published by the WHO in 2024, drug-resistant *Acinetobacter baumannii* is the key first place [3]. Study found that the pathogenesis of *Acinetobacter baumannii* infection is the result of a variety of virulence factors, including porin, capsule and cell wall lipopolysaccharides, enzymes, biofilm production, motility, and iron acquisition systems. These virulence factors work together to cause severe infection in the body [4]. In addition, challenging

and diverse mechanisms of resistance *Acinetobacter baumannii* have been widely recognized, with the major classes of antibiotics being the least effective. Through multiple antibiotic hydrolases, efflux pump variations, impermeability, and antibiotic target mutations, *Acinetobacter baumannii* mimics the unique ability to maintain a multidrug-resistant phenotype, further complicating treatment [5]. Therefore, it is an urgent to screen a highly effective, safe, and with low likelihood of developing drug against MDR-AB.

Previous studies have confirmed that soil is one of the most biodiverse habitats on Earth [6]. Soil microorganisms that survive in extreme environments have evolved extraordinary secondary metabolic capabilities through long-term competition, making them the largest and most successful sources of natural antibacterial compounds [7]. These microorganisms are regarded as potential producers of new antibacterial drugs, including lipopeptide antibiotics, antibacterial compounds, antibacterial peptides, and antibacterial proteins, etc [8]. Among them, antibacterial compounds, especially the natural products and their derivatives produced by microorganisms such as bacteria and fungi, form the basis of modern anti-infective drugs [9]. Particularly notable is their biocompatibility, high antibacterial efficacy, multi-target action mechanism, and high therapeutic index, which have made them important candidate drugs for combating multi-drug resistant pathogens. *Bacillus* is a gram-positive bacterium with a variety of antimicrobial functions, and its antibacterial activity is mainly achieved by producing structurally novel, safe and efficient antibacterial compounds [10]. *Bacillus subtilis*, *Bacillus cereus* and *Bacillus amyloliquefaciens*, as typical spore-forming bacteria, are generally regarded as safe and capable of producing antimicrobial compounds [11]. There have already been several precedents for extracting antibacterial compounds from soil-borne bacillus species [12]. For example, Debois et al. utilized Bacillus FZB42 that can dissolve starch to produce antibiotic compounds, difficidin and bacilysin, which exhibited biocontrol activity against many Pseudomonas species [13]. Podnar et al. demonstrated that *Bacillus subtilis* PS-216 inhibits the growth and biofilm formation of *Salmonella typhimurium* via the production of bacillaene, whose synthesis is dynamically regulated by nutritional conditions and the presence of pathogens [14]. Yu et al. reported that mycosubtilin, a lipopeptide purified from *Bacillus subtilis* ATCC 6633, markedly inhibits the growth of *Fusarium graminearum* PH-1 and *Fusarium verticillioides* 7600 in vitro. It suppresses Candida biofilm formation by up to 95%, disrupts cell membrane integrity, and inhibits hyphal development, exhibiting prominent activity against drug-resistant strains [15].

The purpose of this study was to screen bacteria with antagonistic effects on Multi-drug resistant *Acinetobacter baumannii* (MDR-AB, resistant to aminoglycosides and ampicillin) from microbially rich soil in Changbai Mountain, China. During the screening process, we found that secondary metabolites of *B. subtilis* Y4 had strong antimicrobial activity against Acinetobacter baumannii.Therefore, the antimicrobial substance produced by *B. subtilis* Y4 were separated and purified by n-butanol extraction, silica gel column gradient elution, and RP-HPLC 3-step method, and the antibacterial active component was identified as Oxydifficidin by LC-MS. Its stability to temperature, pH, and enzymes was determined. The antibacterial spectrum, the minimum inhibitory concentration (MIC), and the multi-target antibacterial mechanism against *Acinetobacter baumannii* of Oxydifficidin were studied. And finally, the therapeutic effect on Acinetobact baumannii infecting mice with pneumonia was demonstrated by

transcriptomics and qRT-PCR. This study is the first to conduct an in-depth study on the biological characteristics and in vitro and in vivo antimicrobial mechanism of Oxydifficidin anti-Acinetobacter baumannii, which provides a theoretical basis for its application as a potential natural antimicrobial drug.

2. Materials and methods

2.1 Soil sample collection and isolation of antagonistic bacteria

The antagonistic strain Y4, capable of producing antibacterial compounds, was isolated from microbially rich soil collected in Changbaishan (Baekdusan), Baishan City, Jilin Province, China [16]. Bacterial isolation was performed according to our previously described methods. Briefly, 1 g of soil sample was suspended in 9 mL of sterile water and vortexed for 10 min. The soil suspension was serially diluted to 1×10 − 7. A 100 µL aliquot of the dilution was spread onto Luria–Bertani (LB) agar plates (Sangon Biotech, China) and incubated at 37°C for 12 h in an incubator (ZQPZ-228, Tianjin Leboterui Instrument & Equipment Co., Ltd., China) [17]. Colony morphology on LB agar plates was observed, and single colonies were picked and inoculated into LB broth, followed by incubation at 37°C for 12 h in a shaking incubator (ZQPZ-228, Tianjin Leboterui Instrument & Equipment Co., Ltd., China). Subsequently, a 2.5 µL aliquot of the bacterial culture was spotted onto LB agar plates containing 1×10^6 CFU of MDR-AB, and incubated at 37°C for 12 h in the same incubator (ZQPZ-228, Tianjin Leboterui Instrument & Equipment Co., Ltd., China) [18]. Strains with obvious antagonistic activity against MDR-AB were selected. These strains were inoculated into LB broth at an inoculation volume of 1% and cultured at 37°C for 48 h in a shaking incubator (ZQPZ-228, Tianjin Leboterui Instrument & Equipment Co., Ltd., China) [19]. The culture supernatant was concentrated 10-fold using a rotary evaporator (R502B, SENCO Technology Co., Ltd., China) and filtered through a 0.22 µm membrane filter (Sigma-Aldrich, USA) to obtain cell-free concentrated supernatant. For antibacterial activity evaluation, 200 µL of the cell-free concentrated supernatant was added to LB agar plates containing 1×10^7 CFU of MDR-AB, and incubated at 37°C for 12 h in the incubator (ZQPZ-288, Tianjin Leboterui Instrument & Equipment Co., Ltd., China) [20]. The diameter of the inhibition zone was finally measured and recorded.

2.2 16S rRNA characterization of gene sequences

The genomic DNA of strain Y4 was extracted according to a modified protocol described by Ushida et al. [21]The 16S rRNA gene was amplified by PCR using the universal bacterial primers 27F (5'-AGAGTTTGATCCTGGCTCAG-3') and 1492R (5'-GGHTACCTTGTTACGACTT-3'). The amplification was carried out in a thermal cycler (Bio-Rad, USA). The PCR products were subsequently purified and sequenced. The obtained sequences were compared with reference sequences in the National Center for Biotechnology Information (NCBI) database using the BLAST tool. Multiple sequence alignment was performed using ClustalW. The resulting sequences were submitted to the GenBank database. A phylogenetic tree was then constructed using the neighbor-joining method implemented in Molecular

Evolutionary Genetics Analysis (MEGA) software version 5.0, with bootstrap analysis to assess the robustness of the tree.

2.3 Purification and identification of antibacterial compounds

Strain Y4 was inoculated into LB medium and cultured at 37°C and 180 rpm for 48 h. The cell-free supernatant was obtained by centrifugation at 4°C and 8000 rpm for 20 min using a Sorvall ST1 Plus centrifuge (Thermo Fisher Scientific, USA) [22]. Cell-free supernatant was concentrated 10-fold using a rotary evaporator and extract 2 times with 1 volume of n-butanol and 1 volume of culture filtrate. The n-butanol extract and aqueous phase extract were concentrated under vacuum using a rotary evaporator, respectively [23]. Then, the antibacterial activity of the concentrated solutions of the two was detected by the filter paper method. The crude antibacterial extract was subsequently purified using a silica gel column. Elution was carried out with a stepwise gradient of methanol–ethyl acetate mixtures at ratios of 3:7 (v/v), 5:5 (v/v), and 7:3 (v/v), followed by 100% methanol (1:0, v/v).Each eluate was collected, the antibacterial activity was detected by the filter paper method. The active fraction sample was finally purified by reversed-phase high-performance liquid chromatography (RP-HPLC, Waters 2489, USA) using a Sunfire™ C18 column (19×150 mm, 5 μm,Waters, USA). A 1 mL sample was injected, with the mobile phase consisting of water (0.1% trifluoroacetic acid, Aladdin Biochemical Technology Co., Ltd., China) and acetonitrile (Aladdin Biochemical Technology Co., Ltd., China) [24].

Mass spectrometric analysis was performed using an AB 5600 Triple TOF mass spectrometer (AB Sciex). The flow rate was maintained at 5 mL/min during gradient elution (5%-100%), and monitoring was carried out using a TECAN SPARK UV detector (Switzerland) at 243 nm, with a constant temperature maintained at 28°C. Fractions corresponding to single peaks were collected, freeze-dried into powder using a vacuum freeze dryer (AdVantage Plus, USA), and dissolved with deionized water [25]. The antibacterial activity of the purified each single peaks sample against MDR-AB was assessed using the filtering paper method. Perform primary and secondary mass spectrometry data acquisition based on the information-dependent acquisition (IDA) function under the control of the software Analyst TF 1.7 (AB Sciex), useding LC-ESI-MS analysis of above-mentioned active components [26]. Liquid chromatography was performed on the ACQUITY UPLC HSS T3 Column (2.1 × 100mm; waters, USA) and the column temperature was maintained at 40°C. The mobile phase consists of water (0.1% trifluoroacetic acid, Alad-din Biochemical Technology Co., Ltd., China) and acetoni-trile (Aladdin Biochemical Technology Co., Ltd., China) [27]. To achieve separation, the gradient elution procedure was optimized as follows: Solvent B consisted of 5% for 1.5 min, followed by a linear gradient elution of 5–95% solvent B for 24 min, followed by 95% solvent B for 27 min.The main conditions include the sample injection volume was 4 μL, mass spectra were recorded in negative ion mode with a mass range from m/z 50 to 1200 amu [28]. The electrospray ionization (ESI) source parameters are set to nebulizer gas pressure (GS1) 60 Psi, auxiliary gas pressure 60 Psi, curtain gas pressure 35 Psi, temperature 550°C, spray voltage − 4500V.

2.4 Minimum inhibitory concentration (MIC) assay

The antibacterial spectrum and MIC of oxydifficidin were determined according to our previously described methods [29]. Briefly, the antibacterial compound oxydifficidin was lyophilized, weighed for quantification, and dissolved in PBS (pH = 7.4). The oxydifficidin was diluted to a PBS solution of 1024 μg/mL. For MIC determination, oxydifficidin was subjected to serial two-fold dilutions in PBS, yielding concentrations ranging from 1024 to 1 μg/mL. A volume of 100 μL of each dilution was added to 96-well microplates, followed by the addition of 100 μL of bacterial suspension (1×10^6 CFU/mL) to each well. Wells containing 100 μL of bacterial suspension and 100 μL of Mueller-Hinton (MH) medium without oxydifficidin served as positive growth controls.

All plates were incubated at 37°C for 18 h, and bacterial growth was quantified by measuring the optical density at 600 nm (OD_{600}) using a microplate reader (TECAN SPARK, Switzerland). The MIC was defined as the lowest concentration of oxydifficidin that completely inhibited visible bacterial growth after incubation. All experiments were performed in triplicate, with three independent repeats.

2.5 Stability of the oxydifficidin

The stability of oxydifficidin under different conditions, including temperature, pH, protein hydrolase, and long-term storage, was evaluated according to the method described by Kerek et al. [30].To assess temperature stability, equal concentrations of oxydifficidin samples are treated at constant temperature for 30 min at 28°C, 40°C, 60°C, 80°C, 100°C, separately. In order to evaluate the pH stability, the pH of oxydifficidin was adjusted to 3–9 with 1 mol/L of hydrochloric acid and 1 mol of sodium hydroxide, after 2 h of constant temperature treatment, all samples were adjusted to pH 7.0. For assess protein hydrolase stability, equal amounts of oxydifficidin was separately incubated with 2 mg/mL proteinase K, trypsin, neutral leukin, and alkaline protease solutions at their respective optimal pH levels at 37°C for 2 h, followed by heat treatment at 100°C for 10 min. For storage stability, oxydifficidin was stored at − 80°C, − 20°C, and 4°C for 30 days to evaluate its stability. The antibacterial activity of oxydifficidin after each treatment was determined via the agar diffusion assay against MDR-AB. Untreated oxydifficidin was set as the positive control.

2.6 Scanning electron microscopy(SEM)

MDR-AB(10^6 CFU mL) was incubated with oxydifficidin at 1×MIC at 37°C for 4 h. Cells were then collected by centrifugation (8000 rpm, 4°C, 5 min), washed three times with PBS, and fixed in 2.5% glutaraldehyde(Macklin, China) at 4°C for 12 h. Samples were subsequently dehydrated through a graded ethanol(Aladdin Biochemical Technology Co., Ltd., China) series (30%, 50%, 70%, 80% and 90%). After critical point drying, specimens were sputter-coated and observed using SEM (Hitachi SU8100, Japan) [31].

2.7 Time–kill assay

To evaluate the effect of oxydifficidin on the kinetics of multidrug-resistant MDR-AB, bacterial cultures were adjusted to 10^5 CFU/mL. Oxydifficidin was added at final concentrations of 1×, 2×, and 4×MIC. An equal volume of PBS was added to the control group. Cultures were incubated at 37°C with shaking at

180 rpm for 24 h. Samples were collected at 2 h intervals, and OD_{600} was determined using a microplate reader (Tecan Spark, Switzerland). Time-kill curves were constructed based on OD_{600} values as previously described [32].

2.8 Measurement of nucleic acid and protein leakage

Oxydifficidin at 1×, 2× and 4× MIC was incubated with MDR-AB at 37°C with shaking at 180 rpm for 24 h. The cultures were then centrifuged at 8000 rpm and 4°C for 15 min. The absorbance of the supernatant was measured at 260 nm and 280 nm. OD_{260} and OD_{280} values were used to assess nucleic acid and protein leakage in MDR-AB [33]. This experiment was repeated three times.

2.9 Cytoplasmic membrane permeability

Cytoplasmic membrane permeability was assessed as described by Mwangi et al.. Briefly, MDR-AB cells at the logarithmic growth phase were harvested by centrifugation at 12,000 rpm for 1 min, washed three times with sterile PBS (0.01 M, pH 7.4), and resuspended. Equal volumes of the bacterial suspension were mixed with oxydifficidin at final concentrations of 8–64 μg/mL and incubated at 37°C for 30 min. Subsequently, an equal volume of 10 mM propidium iodide (PI; Aladdin Biochemical Technology Co., Ltd.) was added. Polymyxin B (1μg/mL) was used as a positive control, and PBS as a negative control. Fluorescence intensity was measured at an excitation wavelength of 535 nm and an emission wavelength of 615 nm using a Tecan Spark microplate reader, as previously described [34].

2.10 Outer membrane permeability

Outer membrane permeability was assessed using the 1-N-phenyl-1-naphthylamine (NPN) uptake assay. NPN is a hydrophobic fluorescent probe that exhibits increased fluorescence upon partitioning into lipid environments; thus, an increase in fluorescence intensity reflects enhanced outer membrane permeability. Briefly, MDR-AB cells at the logarithmic growth phase were harvested by centrifugation at 3000 rpm for 10 min, washed three times with PBS, and resuspended in 5 mM HEPES buffer (Sigma-Aldrich, USA). Equal volumes of bacterial suspension and oxydifficidin (8–64 μg/mL) were added to 96-well plates.Polymyxin B and PBS served as positive and negative controls, respectively. Fluorescence intensity was measured using a Tecan Spark microplate reader at an excitation wavelength of 350 nm and an emission wavelength of 420 nm [35].

2.11 Membrane potential

Membrane potential was assessed using the fluorescent probe 3,3'-dipropylthiadicarbocyanine iodide ($DiSC_3(5)$; Sigma-Aldrich, USA). Briefly, MDR-AB cells were cultured to the logarithmic growth phase, harvested by centrifugation at 2500×g and 4°C for 5 min, washed three times with PBS, and resuspended in 5 mM HEPES buffer (Sigma-Aldrich, USA). The bacterial suspension was adjusted to 1×10^7 CFU/mLand aliquoted into 96-well plates.$DiSC_3(5)$ was added to a final concentration of 0.8μM. Oxydifficidin was then added at final concentrations of 8-128 μg/mL, followed by incubation at 37°C for 1 h. Triton X-100 (0.1%) and PBS served as positive and negative controls, respectively. Fluorescence

intensity was measured using a Tecan Spark microplate reader at an excitation wavelength of 622 nm and an emission wavelength of 670 nm [36].

2.12 Biofilm formation

Biofilm inhibition and degradation were assessed using the crystal violet assay. Oxydifficidin was serially twofold diluted to final concentrations of 8-128 μg/mL. MDR-AB cultures were adjusted to 1×10^6 CFU/mL. Equal volumes (50 μL) of oxydifficidin and bacterial suspension were added to each well of a 96-well plate. Following incubation at 37°C for 24 h, the supernatant was removed and the wells were gently washed with sterile water. The adherent biofilm was stained with 1% crystal violet for 30 min, after which the excess stain was removed. The OD_{595} values were measured using a microplate reader (TECAN SPARK, Switzerland) [37].

2.13 Measurement of intracellular reactive oxygen species (ROS)

Intracellular ROS levels were determined using 2',7'-dichlorofluorescein diacetate (DCFH-DA). Bacterial suspensions [38]were adjusted to OD_{600}= 0.6 and incubated with DCFH-DA in the presence of oxydifficidin at final concentrations ranging from 8 to 64 μg/mL. After incubating at 37°C for 30 min, samples were centrifuged at 1,000 rpm for 10 min, washed twice with PBS, and resuspended. Fluorescence intensity was measured using a microplate reader (excitation 488 nm, emission 525 nm; Tecan Spark, Switzerland).

2.14 Safety evaluation

2.14.1 Haemolysis assay

The hemolytic activity of oxydifficidin was evaluated using sterile defibrated sheep erythrocytes [39]. Briefly, 8% (v/v) erythrocyte suspensions were incubated with serial concentrations of oxydifficidin (2-256 μg/mL) at 37°C for 1 h. PBS and 0.2% Triton X-100 were used as negative and positive controls, respectively. Following incubation, samples were centrifuged and the absorbance of the supernatant was measured at 576 nm using a microplate reader (Infinite M200, Tecan). The haemolysis rate was calculated relative to controls.

2.14.2 Mouse safety assessment

A total of 20 mice were randomly assigned to two groups (n = 10 per group): an oxydifficidin-treated group and a control group. Following a 1-week acclimation period, mice in the treatment group received intranasal administration of oxydifficidin at a dose of 10 mg/kg, while control mice received an equal volume of PBS. Animals were monitored for 48 h post-administration. Five mice from each group were randomly selected for blood collection via orbital bleeding for complete blood count analysis. Subsequently, all mice were euthanized, and major organs (heart, liver, spleen, lung and kidney) were harvested for histopathological examination following haematoxylin and eosin (H&E) staining [40]. All

mice tests were carried out in accordance with the Regulations for Animal Experimentation at Jilin Agricultural University (JLAU08201409) and Laboratory Animal Care and Use Guidelines of National Institutes of Health (NIH Publication No. 8023).

2.15 Neutropenic mouse pneumonia model

Male BALB/c mice (20–22 g) were used to establish a mouse pneumonia model. Mice were rendered immunosuppressed by intraperitoneal injection of cyclophosphamide (150 mg/kg) for three consecutive days, followed by inoculation with 1×10^9 colony-forming units (CFU) of MDR-AB. Animals were randomly assigned to three groups (n = 15 per group): a control group, a model group, and a treatment group. The control group received immunosuppression only without MDR-AB infection, whereas the model and treatment groups were subjected to the MDR-AB pneumonia model according to the established protocol. At 1 h post-infection, mice in the treatment group received intranasal administration of oxydifficidin (20 μL, 10 mg/kg), while mice in the model and control groups received an equal volume of sterile PBS. All mice were euthanized 24 h after infection, and major organs were collected. Lung tissues were homogenized to determine bacterial burden. In addition, lung, heart, liver, spleen, and kidney tissues were fixed in 4% paraformaldehyde, embedded in paraffin, sectioned, and subjected to haematoxylin and eosin (H&E) staining for histopathological examination. Body weight was recorded daily throughout the experiment [41].

2.16 Serum inflammatory cytokine measurement and lung tissue gene expression analysis

2.16.1 Serum cytokine analysis

At 24 h post-infection, blood samples were collected and allowed to clot at room temperature for 30 min. Serum was obtained by centrifugation at 3,500 rpm for 10 min. Levels of TNF-α, IL-1β, and IL-6 were quantified using commercial ELISA kits according to the manufacturer's instructions [42].

2.16.2 RNA sequencing and transcriptom ic analysis

Total RNA was extracted from mouse lung tissues of the three experimental groups using TRIzol reagent, with three biological replicates per group. Transcriptomic analysis was performed using next-generation sequencing (NGS) on an Illumina platform (Personalbio Biotechnology Co., Ltd., Shanghai, China). Differential expression analysis was conducted using the DESeq2 package. Differentially expressed genes (DEGs) were identified based on the thresholds of $|\log_2\text{FoldChange}| > 1$ and adjusted p-value (padj) < 0.05. Functional enrichment analyses of DEGs, including Gene Ontology (GO) and Kyoto Encyclopedia of Genes and Genomes (KEGG), were performed using the ClusterProfiler package. Enrichment results were visualized using bubble plots [43].

2.16.3 RT–qPCR analysis

Total RNA from lung tissues was extracted and reverse-transcribed into cDNA using a commercial kit. Quantitative PCR was performed using SYBR Green chemistry in a 20 μL reaction volume. Gene

expression levels of IL-6, IL-1β, TNF-α, and other target genes were determined. GAPDH was used as the internal reference gene [44]. Relative expression levels were calculated using the $2^{-\Delta\Delta Ct}$ method. Primer sequences are listed in Supplementary Table 1.

2.17 Statistical analysis

All experiments were performed in triplicate, and data are presented as mean ± SD. Statistical analysis was conducted using SPSS v.22.0, with one-way ANOVA or MANOVA as appropriate, followed by Tukey's post hoc test. Differences were considered significant at $*p < 0.05$ and highly significant at $***p < 0.001$.

3. Results

3.1 Isolation and Identification of the Antibacterial Strain *Bacillus subtilis* Y4

A bacterial strain exhibiting strong antagonistic activity against MDR-AB was isolated from the soil samples collected in Changbaishan (Supplementary Fig. 1A). Colonies of strain Y4 were round with irregular surface folds and a milky-white appearance (Supplementary Fig. 1B). Phylogenetic analysis based on the 16S rRNA gene sequence showed 99% similarity to *Bacillus velezensis* NRRL B-41580 (Supplementary Fig. 1C), indicating that strain Y4 belongs to *Bacillus subtilis*.

3.2 Isolation and Structural Characterization of the Antibacterial Compound Oxydifficidin

The n-butanol extract of strain Y4 exhibited strong antibacterial activity against MDR-AB as determined by the filter paper diffusion method. Subsequent purification by silica gel column chromatography using a methanol/ethyl acetate gradient (7:3, v/v) yielded a single active fraction. Further purification by preparative RP-HPLC produced six peaks, among which only the fifth peak exhibited antibacterial activity (Fig. 1A). LC-MS analysis revealed a molecular ion peak at m/z 559.28925 ([M-H]-), corresponding to a molecular formula of C31H44O7P (Supplementary Fig. 2). The UV absorption spectrum showed characteristic peaks at 235 nm and 273 nm, consistent with previously reported oxydifficidin [45]. MS/MS analysis further demonstrated that the major fragment ions matched the reported fragmentation pattern, with mass deviations below 8 ppm (Supplementary Table 2). Based on these results, the antibacterial compound was identified as oxydifficidin.

3.3 Stability Characterization of Oxydifficidin Under Different Conditions

The stability of oxydifficidin under different conditions was evaluated. As shown in Supplementary Table 3, oxydifficidin retained 85.1% of its antibacterial activity after treatment at 60°C for 30 min. Oxydifficidin showed no detectable activity under strongly acidic conditions (pH = 3), maintained relatively stable activity at near-neutral (pH = 7), and exhibited reduced activity under alkaline conditions

(pH > 8). Regarding enzymatic stability, oxydifficidin was relatively resistant to neutral and alkaline proteases, while pepsin moderately reduced its activity. Additionally, oxydifficidin retained over 90% of its activity after storage at -80°C for 30 days (Supplementary Fig. 3).

3.4 Antibacterial Activity of Oxydifficidin Against Pathogenic Bacteria

The antibacterial activity of oxydifficidin against a range of Gram-positive and Gram-negative bacteria was evaluated by determining the MIC (Supplementary Table 4). The results demonstrated that oxydifficidin exhibited broad-spectrum antimicrobial activity, with an MIC of 16 μg/mL against MDR-AB.

3.5 Time-Dependent Bactericidal Activity of Oxydifficidin

Time-kill assays demonstrated that oxydifficidin inhibited bacterial growth in a concentration-dependent manner (Fig. 1B). At 1×MIC, bacterial growth was significantly suppressed, with the OD_{600} at 24 h reduced to approximately half that of the control. At 2×MIC, bacterial growth remained at a consistently low level throughout the incubation period. In contrast, treatment with 4×MIC oxydifficidin resulted in rapid and sustained bactericidal activity, with MDR-AB showing almost no further growth.

3.6 Oxydifficidin Disrupts Bacterial Membrane Integrity Leading to Cellular Leakage

To further evaluate the disruptive effect of oxydifficidin on membrane integrity, the leakage of intracellular macromolecules, including nucleic acids and proteins, was measured in MDR-AB cultures treated with different concentrations of oxydifficidin. As shown in Fig. 2A and B, both nucleic acid and protein leakage increased in a concentration-dependent manner. When the concentration of oxydifficidin increased from 8 to 64 μg/mL, the extracellular levels of nucleic acids and proteins increased by 11% and 23%, respectively, compared with the control.

3.7 Oxydifficidin Increases Bacterial Membrane Permeability

Cytoplasmic membrane damage was assessed using propidium iodide (PI), a membrane-impermeable nucleic acid stain. As shown in Fig. 2C, compared with the PBS control, cytoplasmic membrane permeability of MDR-AB increased progressively with increasing concentrations of oxydifficidin, indicating that higher concentrations significantly compromise membrane integrity ($p < 0.0001$). Outer membrane permeability was further evaluated using the hydrophobic fluorescent probe 1-N-phenyl-1-naphthylamine (NPN). As shown in Fig. 2D, NPN fluorescence intensity increased markedly in a concentration-dependent manner, demonstrating that oxydifficidin effectively disrupts the outer membrane structure of MDR-AB cells.

3.8 Oxydifficidin Induces Membrane Depolarization in Bacterial Cells

Changes in membrane polarization were assessed using the fluorescent probe DiSC3(5). As shown in Fig. 3A, oxydifficidin induced rapid and concentration-dependent depolarization of the membrane potential in MDR-AB cells, with a highly significant effect ($p < 0.0001$).

3.9 Oxydifficidin Inhibits Biofilm Formation of Bacterial Pathogens

As shown in Fig. 2E, oxydifficidin significantly inhibited biofilm formation in MDR-AB compared with the PBS control ($p < 0.0001$), with a clear dose-dependent effect. This finding indicates that oxydifficidin interferes with biofilm development, which is closely associated with bacterial persistence and resistance.

3.10 Oxydifficidin Induces Intracellular Reactive Oxygen Species Accumulation

Intracellular reactive oxygen species (ROS) levels were measured using the fluorescent probe DCFH-DA. As shown in Fig. 3B, treatment with oxydifficidin at different concentrations resulted in a concentration-dependent increase in fluorescence intensity in MDR-AB cells, indicating enhanced ROS accumulation. Notably, ROS levels reached a peak after 60 min of treatment with 64 μg/mL oxydifficidin ($p < 0.0001$).

3.11 Evaluation of the Biosafety Profile of Oxydifficidin

Oxydifficidin exhibited low haemolytic activity against red blood cells across the tested concentration range. At concentrations up to 64 μg/mL (4×MIC), the haemolysis rate remained below 10%, indicating minimal haemolytic effects within the effective antimicrobial range (Fig. 3C).

Following intraperitoneal administration of oxydifficidin at 10 mg/kg, no significant abnormalities in behaviour, food intake, or activity were observed in mice, and no mortality occurred during the 7-day observation period. Haematological analysis (Supplementary Table 5) showed that all measured parameters were within normal ranges and did not differ significantly from those of the control group, suggesting that oxydifficidin does not induce detectable systemic toxicity at this dosage.

Furthermore, after 7 days of intranasal administration, major organs-including the heart, liver, spleen, lung, and kidney-were collected for haematoxylin and eosin (H&E) staining (Supplementary Fig. 4). Histological examination revealed normal tissue architecture in the oxydifficidin-treated group, with no significant differences compared with the control. These findings indicate that oxydifficidin does not cause evident damage to major organs under the tested conditions. Collectively, oxydifficidin demonstrates favourable safety profiles both in vitro and in vivo.

3.12 Oxydifficidin Protects Against Multidrug-Resistant Acinetobacter baumannii-Induced Pneumonia in Mice

An immunocompromised mouse model was established by intraperitoneal administration of cyclophosphamide, followed by intratracheal inoculation with a non-lethal dose of MDR-AB (10^9CFU) to induce pneumonia. During model establishment, peripheral blood analysis showed significant reductions in white blood cells, lymphocytes, and granulocytes, all falling well below normal reference ranges. This marked decrease in immune cell counts indicates successful immunosuppression. Combined with the observed body weight decline, these findings confirm the successful establishment of the immunocompromised model (Supplementary Fig. 5A and B).

Treatment was initiated 1 h post-infection, and samples were collected at 24 h for analysis. Compared with the model group, oxydifficidin treatment reduced the bacterial load in lung tissues by 2.30 $\log_{10}$CFU/g, demonstrating potent in vivo antibacterial activity (Fig. 4A).

In addition, gross pathological examination revealed that oxydifficidin treatment alleviated lung inflammation, as evidenced by reduced hyperaemia and fewer haemorrhagic spots. Overall lung lesions were markedly attenuated compared with the infected group, indicating that oxydifficidin mitigates MDR-AB-induced lung injury (Fig. 4B).

Furthermore, oxydifficidin significantly decreased serum levels of pro-inflammatory cytokines, including IL-6, IL-1β, and TNF-α (Fig. 4C-E), suggesting effective suppression of the systemic inflammatory response induced by MDR-AB infection.

3.13 Transcriptomic Profiling Reveals Differential Gene Expression After Oxydifficidin Treatment

Using $|\log_2 FC| > 1$ and adjusted p-value (padj) < 0.05 as the thresholds for differential expression analysis, a total of 1,760 differentially expressed genes (DEGs) were identified in the control group compared with the model group, including 1,068 upregulated and 692 downregulated genes (Fig. 5A). In comparison with the model group, 1,578 DEGs were identified in the oxydifficidin-treated group, of which 1,076 were upregulated and 502 were downregulated (Fig. 5B).Volcano plot analysis (Fig. 5C and D) further illustrated the global distribution of DEGs in terms of fold change and statistical significance, demonstrating that oxydifficidin treatment markedly altered the overall gene expression profile. Functional enrichment analysis revealed that these DEGs were primarily associated with cell membrane structure, transport systems, and cell envelope-related processes, highlighting the bacterial cell envelope as a potential key target. These findings suggest that oxydifficidin may impair membrane integrity and disrupt transport processes, thereby weakening the permeability barrier of bacterial cells.

Hierarchical clustering analysis (Fig. 5E) showed clear separation of gene expression patterns among different groups, indicating that oxydifficidin treatment significantly reshaped the expression profile of membrane-associated genes. Meanwhile, Pearson correlation analysis (Fig. 5F) demonstrated high consistency among biological replicates within each group ($r > 0.97$), confirming the reliability of the

RNA-seq data and further supporting the presence of substantial transcriptional differences between groups.

Combined with functional evidence of membrane depolarization and leakage of intracellular components, the transcriptomic data further confirm at the molecular level that oxydifficidin exerts its antibacterial activity by disrupting membrane integrity and disturbing cell envelope homeostasis, ultimately leading to bacterial cell death.

3.14 Oxydifficidin Modulates Immune and Inflammatory Responses Revealed by Transcriptomic Analysis

GO and KEGG enrichment analyses (Fig. 5G and H) consistently demonstrated that the differentially expressed genes were primarily involved in immune response and host defense processes. Among the enriched pathways, the complement and coagulation cascades showed the highest degree of enrichment, indicating their critical role in the host response to multidrug-resistant Acinetobacter baumannii (MDR-AB) infection. In the model group, excessive activation of the complement system accompanied by enhanced cytokine signaling reflected an aberrant immune response characterized by hyperinflammation and immune imbalance. Although these immune responses contribute to pathogen clearance, their sustained or excessive activation can exacerbate tissue damage and promote the progression of severe pneumonia.

Importantly, oxydifficidin treatment significantly modulated these immune-related pathways. By suppressing excessive complement activation and attenuating cytokine–receptor interactions and chemokine signaling pathways, oxydifficidin effectively alleviated inflammatory responses while preserving essential host defense functions. These findings suggest that the therapeutic effects of oxydifficidin are not solely attributable to its direct antibacterial activity but are also closely associated with its ability to regulate host immune homeostasis. Through the coordinated modulation of complement activity and cytokine signaling pathways, oxydifficidin may reduce inflammation-associated tissue injury while promoting pathogen clearance during MDR-AB-induced pneumonia.[46].

3.15 qRT-PCR Validation of Transcriptomic Data in Lung Tissues

The ELISA results indicated that oxydifficidin regulates the protein levels of TNF-α, IL-6 and IL-1β. To determine whether this regulatory effect also occurs at the transcriptional level, we further examined mRNA expression using qRT-PCR. MDR-AB infection markedly increased the mRNA levels of TNF-α, IL-6 and IL-1β in mouse lung tissues, whereas oxydifficidin treatment reduced these elevations to varying degrees (Fig. 6A-C). These findings suggest that oxydifficidin modulates the MDR-AB-induced inflammatory response at both transcriptional and translational levels.To further validate the transcriptomic data, three genes were randomly selected for qRT-PCR analysis. As shown in Fig. 6D, the

expression patterns were consistent with those observed in the transcriptomic dataset, supporting the reliability of the sequencing results.

4. Discussion

The emergence of MDR-AB has significantly limited the effectiveness of current antimicrobial therapies [47],T highlighting the urgent need for novel antimicrobial agents with distinct mechanisms of action. Microorganisms from competitive ecological environments, particularly soil-derived bacteria, represent valuable sources of bioactive secondary metabolites [48].

In this study, *B. subtilis* Y4 isolated from Changbai Mountain soil was identified as a promising producer of antimicrobial metabolites. Through bioassay-guided purification and LC-HRMS analysis, oxydifficidin, a difficidin-family polyketide derivative [49], was identified as the major active compound responsible for the antibacterial activity against MDR-AB. Previous studies have demonstrated that oxydifficidin exhibits antibacterial activity against several Gram-negative pathogens [50]; however, its activity against MDR-AB and underlying mechanisms remain largely unexplored. Our findings provide the first systematic evidence that oxydifficidin exhibits potent antibacterial activity against MDR-AB and possesses therapeutic potential in an infection model.The stability and biosafety of antimicrobial compounds are critical factors for further development. Oxydifficidin exhibited favorable physicochemical stability, maintaining antibacterial activity under moderate temperature and neutral pH conditions. In addition, its low hemolytic activity and absence of obvious toxicity in mice indicate acceptable biological compatibility, supporting its potential application as an antimicrobial candidate. Previous studies have similarly demonstrated that the stability of polymyxin antibiotics is strongly influenced by environmental pH, temperature, and enzymatic degradation [51]. Therefore, the stability profile of oxydifficidin may be closely associated with its chemical structure and surrounding physicochemical conditions.

Mechanistic investigations revealed that oxydifficidin exerted a multi-target antibacterial effect primarily associated with bacterial membrane disruption. Oxydifficidin increased outer membrane permeability, induced membrane depolarization, and promoted leakage of intracellular macromolecules, suggesting disruption of membrane integrity and energy metabolism. Furthermore, oxydifficidin induced intracellular ROS accumulation, which may amplify bacterial damage caused by membrane dysfunction. In addition, oxydifficidin significantly inhibited biofilm formation, indicating potential anti-virulence activity against MDR-AB. The combination of membrane targeting, oxidative stress induction, and biofilm inhibition may contribute to its potent antibacterial activity and reduce the likelihood of rapid resistance development. This action mode is highly consistent with the characteristics of membrane-targeted and metabolism-inhibited antimicrobial substances summarized by Benfield AH et al. [52].

The therapeutic efficacy of oxydifficidin was further confirmed in an immunosuppressed mouse model of MDR-AB-induced pneumonia. Oxydifficidin treatment significantly decreased bacterial burden in lung tissues and alleviated pathological damage, including inflammatory infiltration and tissue injury. Since MDR-AB-associated disease severity is closely linked to excessive host inflammatory responses,

modulation of inflammation represents an important component of effective therapy [53]. Oxydifficidin reduced the expression of pro-inflammatory cytokines, including TNF-α, IL-1β, and IL-6, suggesting that its protective effects may result from both bacterial clearance and attenuation of infection-associated inflammation.

Transcriptomic analysis further demonstrated that oxydifficidin treatment regulated immune-related pathways, particularly complement and coagulation cascades and cytokine–cytokine receptor interactions. These findings suggest that oxydifficidin may alleviate MDR-AB-induced lung injury by reducing bacterial stimulation and restoring immune homeostasis. However, further studies are required to clarify its direct molecular targets, pharmacokinetic characteristics, and potential for resistance development.

In conclusion, this study identifies oxydifficidin derived from *B. subtilis* Y4 as a promising antimicrobial metabolite against MDR-AB. Oxydifficidin exhibits potent antibacterial activity through multiple mechanisms, including membrane disruption, ROS induction, and biofilm inhibition, and demonstrates therapeutic efficacy and biosafety in vivo. These findings provide a foundation for the further development of oxydifficidin as a potential antimicrobial agent against multidrug-resistant bacterial infections.

5. Conclusion

In this study, we identified oxydifficidin, a bioactive compound produced by *B. subtilis* Y4, which exhibits broad-spectrum antibacterial activity against both Gram-positive and Gram-negative bacteria. Mechanistic studies demonstrated that oxydifficidin disrupts bacterial membrane integrity, induces oxidative stress, and inhibits biofilm formation, ultimately leading to bacterial death. In vivo, oxydifficidin significantly reduced bacterial burden and alleviated lung injury, while modulating pro-inflammatory cytokines such as TNF-α, IL-1β, and IL-6, suggesting a potential role in host immune regulation. Despite these promising findings, the precise molecular targets and pharmacokinetic properties of oxydifficidin remain to be further investigated. Overall, our findings provide strong evidence for the antibacterial and immunomodulatory potential of oxydifficidin, highlighting its promise as a lead candidate for the development of novel therapeutics against multidrug-resistant bacterial infections.

Declarations

Competing Interests The authors declare no competing interests.

CRediT authorship contribution statement Xinyuan Li and Haowen Yan: Writing – original draft, Visualization, Validation, Meth-odology, Data curation.Jinyu Mou: Writing – review & editing, Investigation. Jinyang Gu: Investigation, Formal analysis. Lili Guan and Jingrui Chen: Formal analysis,Investigation. Lingcong Kong: Formal analysis.Haipeng Zhang and Hongxia Ma: Conceptualization,Funding acquisition,Methodology,Writing – review & editing.

Funding This work was supported by the National Natural Science Foundation of China [grant numbers 32302932, 32473097]; the National Natural Science Foundation Regional Innovation and Development Joint fund of China [grant number U23A20242]; and the Jilin Province Science and Technology Development Plan Project [grant number 20260203105SF].

Data Availability The datasets used and/or analyzed during the current study are available from the corresponding author on reasonable request.

Ethics approval The animal study protocol was approved by the Laboratory Animal Ethics Committee of Jilin Agricultural University (protocol code 20250827008 and the approval date is August 27, 2025).

References

1. Vahhabi A, Hasani A, Rezaee MA, Baradaran B, Hasani A, Samadi Kafil H, et al. A plethora of carbapenem resistance in Acinetobacter baumannii: no end to a long insidious genetic journey. Journal of Chemotherapy. 2020. doi: 10.1080/1120009x.2020.1847421.
2. Ibrahim S, Al-Saryi N, Al-Kadmy IMS, Aziz SN. Multidrug-resistant Acinetobacter baumannii as an emerging concern in hospitals. Molecular Biology Reports. 2021. doi: 10.1007/s11033-021-06690-6.
3. Mohammadi F, Karami P, Arabestani MR, Khaledi A, Alikhani MY. Molecular Typing of Clinical Isolates of Acinetobacter baumannii Using Random Amplified Polymorphic DNA (RAPD-PCR). Iranian Journal of Public Health. 2021. doi: 10.18502/ijph.v50i4.6019.
4. Choi G, Choi SH. Complex regulatory networks of virulence factors in Vibrio vulnificus. Trends in Microbiology. 2022. doi: 10.1016/j.tim.2022.05.009.
5. Ayoub Moubareck C, Hammoudi Halat D. Insights into Acinetobacter baumannii: A Review of Microbiological, Virulence, and Resistance Traits in a Threatening Nosocomial Pathogen. Antibiotics. 2020. doi: 10.3390/antibiotics9030119.
6. Thakur MP, Phillips HRP, Brose U, De Vries FT, Lavelle P, Loreau M, et al. Towards an integrative understanding of soil biodiversity. Biological Reviews. 2019. doi: 10.1111/brv.12567.
7. Mullis MM, Rambo IM, Baker BJ, Reese BK. Diversity, Ecology, and Prevalence of Antimicrobials in Nature. Frontiers in Microbiology. 2019. doi: 10.3389/fmicb.2019.02518.
8. Sreelakshmi KP, Madhuri M, Swetha R, Rangarajan V, Roy U. Microbial lipopeptides: their pharmaceutical and biotechnological potential, applications, and way forward. World Journal of Microbiology and Biotechnology. 2024. doi: 10.1007/s11274-024-03908-0.
9. Rahman MM, Rahaman MS, Islam MR, Hossain ME, Mannan Mithi F, Ahmed M, et al. Multifunctional Therapeutic Potential of Phytocomplexes and Natural Extracts for Antimicrobial Properties. Antibiotics. 2021. doi: 10.3390/antibiotics10091076.
10. Fira D, Dimkić I, Berić T, Lozo J, Stanković S. Biological control of plant pathogens by Bacillus species. Journal of Biotechnology. 2018. doi: 10.1016/j.jbiotec.2018.07.044.

11. Lee N-K, Kim W-S, Paik H-D. Bacillus strains as human probiotics: characterization, safety, microbiome, and probiotic carrier. Food Science and Biotechnology. 2019. doi: 10.1007/s10068-019-00691-9.
12. Waongo B, Ndayishimiye L, Tapsoba F, Zongo W-SA, Li J, Savadogo A. Prospection for potential new non-ribosomal peptide gene clusters in Bacillus genus isolated from fermented foods and soil through genome mining. Frontiers in Microbiology. 2025. doi: 10.3389/fmicb.2025.1515483.
13. Debois D, Ongena M, Cawoy H, De Pauw E. MALDI-FTICR MS Imaging as a Powerful Tool to Identify Paenibacillus Antibiotics Involved in the Inhibition of Plant Pathogens. Journal of the American Society for Mass Spectrometry. 2013. doi: 10.1007/s13361-013-0620-2.
14. Podnar E, Erega A, Danevčič T, Kovačec E, Lories B, Steenackers H, et al. Nutrient Availability and Biofilm Polysaccharide Shape the Bacillaene-Dependent Antagonism of Bacillus subtilis against Salmonella Typhimurium. Microbiology Spectrum. 2022. doi: 10.1128/spectrum.01836-22.
15. Yu C, Liu X, Zhang X, Zhang M, Gu Y, Ali Q, et al. Mycosubtilin Produced by Bacillus subtilis ATCC6633 Inhibits Growth and Mycotoxin Biosynthesis of Fusarium graminearum and Fusarium verticillioides. Toxins. 2021. doi: 10.3390/toxins13110791.
16. Yang K, Dai X, Maitikadir Z, Zhang H, Hao H, Yan C. Comparative genome analysis of endophytic Bacillus amyloliquefaciens MR4: a potential biocontrol agent isolated from wild medicinal plant root tissue. Journal of Applied Genetics. 2024. doi: 10.1007/s13353-024-00905-9.
17. Almasi F, Kafshnouchi M, Mohammadipanah F, Hamedi J. Fruit wrapping kraft coated paper promotes the isolation of actinobacteria using ex situ and in situ methods. Folia Microbiologica. 2021. doi: 10.1007/s12223-021-00907-8.
18. Thi Vu H, Otsuka S, Ueda H, Senoo K. Cocultivated bacteria can increase or decrease the culture lifetime of Chlorella vulgaris. The Journal of General and Applied Microbiology. 2010. doi: 10.2323/jgam.56.413.
19. Chen F, Wang L, Wang M, Xie Y, Xia X, Li X, et al. Genetic characterization and in vitro activity of antimicrobial combinations of multidrug-resistant Acinetobacter baumannii from a general hospital in China. Oncology Letters. 2018. doi: 10.3892/ol.2017.7600.
20. Hwang S, Choi J. Rapid antimicrobial susceptibility testing for low bacterial concentrations integrating a centrifuge based bacterial cell concentrator. Lab on a Chip. 2022. doi: 10.1039/d2lc00974a.
21. Ushida K, Segawa T, Kohshima S, Takeuchi N, Fukui K, Li Z, et al. Application of real-time PCR array to the multiple detection of antibiotic resistant genes in glacier ice samples. The Journal of General and Applied Microbiology. 2010. doi: 10.2323/jgam.56.43.
22. Ding X, Qian F, Mu G, Tuo Y. Optimization of medium composition of Lactobacillus plantarum Y44 using Plackett–Burman and Box–Behnken designs. Preparative Biochemistry & Biotechnology. 2023. doi: 10.1080/10826068.2023.2166957.
23. McNamara RP, Caro-Vegas CP, Costantini LM, Landis JT, Griffith JD, Damania BA, et al. Large-scale, cross-flow based isolation of highly pure and endocytosis-competent extracellular vesicles. Journal

of Extracellular Vesicles. 2018. doi: 10.1080/20013078.2018.1541396.

24. Majouli K, Hamdi A, Msaada K, Kenani A. A bioactivity guided study on the antibacterial activity of Hertia cheirifolia L. extracts. Microbial Pathogenesis. 2016. doi: 10.1016/j.micpath.2016.10.015.
25. Verstraeten M, Broeckhoven K, Lynen F, Choikhet K, Dittmann M, Witt K, et al. Comparison of the quantitative performance of constant pressure versus constant flow rate gradient elution separations using concentration-sensitive detectors. Journal of Chromatography A. 2011. doi: 10.1016/j.chroma.2011.10.019.
26. Mkhize B, Court R, Castel S, Joubert A, van der Merwe M, Wiesner L. Development and validation of a liquid chromatography tandem mass spectrometry assay for the analysis of bedaquiline and M2 in breast milk. Journal of Mass Spectrometry and Advances in the Clinical Lab. 2023. doi: 10.1016/j.jmsacl.2023.12.001.
27. Pietrogrande MC, Dondi F, Ciogli A, Gasparrini F, Piccin A, Serafini M. Characterization of new types of stationary phases for fast and ultra-fast liquid chromatography by signal processing based on AutoCovariance Function: A case study of application to Passiflora incarnata L. extract separations. Journal of Chromatography A. 2010. doi: 10.1016/j.chroma.2010.04.048.
28. Rotkaja O, Golushko J, Mekss P. Behaviour of proteins on reversed-phase supports during high performance liquid chromatography on C18 stationary phase. Proceedings of the Estonian Academy of Sciences. 2015. doi: 10.3176/proc.2015.1.05.
29. Almatrood W, Nakouti I, Hobbs G. Microtiter plate with built-in oxygen sensors: a novel approach to investigate the dynamics of Pseudomonas aeruginosa growth suppression in the presence of divalent cations and antibiotics. Archives of Microbiology. 2022. doi: 10.1007/s00203-022-02877-y.
30. Kerek Á, Ecsedi BG, Szabó Á, Szimrók Z, Paliczné Kustán B, Jerzsele Á, et al. Stability Studies of the Dilution Series of Different Antibiotic Stock Solutions in Culture Medium Incubated at 37 °C. Antibiotics. 2024. doi: 10.3390/antibiotics13060549.
31. Kolpen M, Jensen PØ, Qvist T, Kragh KN, Ravnholt C, Fritz BG, et al. Biofilms of Mycobacterium abscessus Complex Can Be Sensitized to Antibiotics by Disaggregation and Oxygenation. Antimicrobial Agents and Chemotherapy. 2020. doi: 10.1128/aac.01212-19.
32. Singh S, Gumbo T, Boorgula GD, Thomas TA, Philley JV, Srivastava S. Omadacycline pharmacokinetics/pharmacodynamics and efficacy against multidrug-resistant Mycobacterium tuberculosis in the hollow fiber system model. Antimicrobial Agents and Chemotherapy. 2023. doi: 10.1128/aac.01080-23.
33. Lin H, Zhou C, Yu K-H, Lin Y-S, Wang L-B, Zhang Y, et al. Glabridin Functions as a Quorum Sensing Inhibitor to Inhibit Biofilm Formation and Swarming Motility of Multidrug-Resistant Acinetobacter baumannii. Infection and Drug Resistance. 2023. doi: 10.2147/idr.s417751.
34. Nitsch A, Haralambiev L, Einenkel R, Muzzio DO, Zygmunt MT, Ekkernkamp A, et al. Determination of In Vitro Membrane Permeability by Analysis of Intracellular and Extracellular Fluorescein Signals in Renal Cells. In Vivo. 2019. doi: 10.21873/invivo.11667.

35. Sakalauskaitė S, Mikalayeva V, Sutkuvienė S, Daugelavičius R. Mode of the Interaction of Efflux Inhibitor Phenylalanyl-arginyl-β-naphtylamide with Bacterial Cells. Biomedicines. 2024. doi: 10.3390/biomedicines12061324.
36. Prashar S, Portales Guemes M, Shivbaran P, Jimenez Alvarez E, Soha C, Nacer S, et al. Novel Disk Diffusion Assay on Magnesium Oxalate Agar To Evaluate the Susceptibility of Yersinia pestis to Type III Secretion System Inhibitors. Microbiology Spectrum. 2021. doi: 10.1128/spectrum.00005-21.
37. Andersen JB, Rybtke M, Tolker-Nielsen T. The dynamics of biofilm development and dispersal should be taken into account when quantifying biofilm via the crystal violet microtiter plate assay. Biofilm. 2024. doi: 10.1016/j.bioflm.2024.100207.
38. Figueroa D, Asaduzzaman M, Young F. Real time monitoring and quantification of reactive oxygen species in breast cancer cell line MCF-7 by 2',7'-dichlorofluorescin diacetate (DCFDA) assay. Journal of Pharmacological and Toxicological Methods. 2018. doi: 10.1016/j.vascn.2018.03.007.
39. Jiang N, Wang T, Fang Y, Liu X, Dai N, Ruan H, et al. A Novel Protein Demonstrating Antibacterial Activity Against Multidrug-Resistant Escherichia coli Purified from Bacillus velezensis CB6. Foods. 2025. doi: 10.3390/foods14071255.
40. Chen Z-y, Lin Y-m, Wu J-h, Zhang X-q, Zhang Y, Xie W-x, et al. Effect of doxofylline on pulmonary inflammatory response and oxidative stress during mechanical ventilation in rats with COPD. BMC Pulmonary Medicine. 2022. doi: 10.1186/s12890-022-01859-6.
41. Malcolm KC, Ochoa AE, Congel JH, Hume PS, Corley JM, Wheeler EA, et al. A Murine Model of Mycobacterium abscessus Infection Mimics Pathology of Chronic Human Lung Disease. American Journal of Respiratory Cell and Molecular Biology. 2025. doi: 10.1165/rcmb.2024-0376le.
42. Tümer KÇ, Kızıl M. Circulatory cytokines during the piroplasm stage of natural Theileria annulata infection in cattle. Parasite Immunology. 2023. doi: 10.1111/pim.12973.
43. Pennitz P, Kirsten H, Friedrich VD, Wyler E, Goekeri C, Obermayer B, et al. A pulmonologist's guide to perform and analyse cross-species single lung cell transcriptomics. European Respiratory Review. 2022. doi: 10.1183/16000617.0056-2022.
44. Fragoulis A, Biller K, Fragoulis S, Lex D, Uhlig S, Reiss LK. Reference Gene Selection for Gene Expression Analyses in Mouse Models of Acute Lung Injury. International Journal of Molecular Sciences. 2021. doi: 10.3390/ijms22157853.
45. Im SM, Yu NH, Joen HW, Kim SO, Park HW, Park AR, et al. Biological control of tomato bacterial wilt by oxydifficidin and difficidin-producing Bacillus methylotrophicus DR-08. Pesticide Biochemistry and Physiology. 2020. doi: 10.1016/j.pestbp.2019.11.007.
46. Hermanns HM, Wohlfahrt J, Mais C, Hergovits S, Jahn D, Geier A. Endocytosis of pro-inflammatory cytokine receptors and its relevance for signal transduction. Biological Chemistry. 2016. doi: 10.1515/hsz-2015-0277.
47. Alenazi TA, Shaman MSB, Suliman DM, Alanazi TA, Altawalbeh SM, Alshareef H, et al. The Impact of Multidrug-Resistant Acinetobacter baumannii Infection in Critically Ill Patients with or without

COVID-19 Infection. Healthcare. 2023. doi: 10.3390/healthcare11040487.

48. Geers AU, Buijs Y, Strube ML, Gram L, Bentzon-Tilia M. The natural product biosynthesis potential of the microbiomes of Earth – Bioprospecting for novel anti-microbial agents in the meta-omics era. Computational and Structural Biotechnology Journal. 2021. doi: 10.1016/j.csbj.2021.12.024.
49. Zimmerman, B S, Schwartz, D C, Monaghan, L R, et al. Difficidin and oxydifficidin: novel broad spectrum antibacterial antibiotics produced by Bacillus subtilis. I. Production, taxonomy and antibacterial activity. The Journal of Antibiotics. 1987.
50. Nie F, Yan J, Ling Y, Liu Z, Fu C, Li X, et al. Effect of Shuangdan Mingmu capsule, a Chinese herbal formula, on oxidative stress-induced apoptosis of pericytes through PARP/GAPDH pathway. BMC Complementary Medicine and Therapies. 2021. doi: 10.1186/s12906-021-03238-w.
51. Yadav A, Sathala P, Divate M, Chenkul L, Nupur N, Upmanyu N, et al. Deciphering solid state photostability of polymyxin B using deconvolution based FTIR insights. Spectrochimica Acta Part A: Molecular and Biomolecular Spectroscopy. 2025. doi: 10.1016/j.saa.2025.126256.
52. Benfield AH, Henriques ST. Mode-of-Action of Antimicrobial Peptides: Membrane Disruption vs. Intracellular Mechanisms. Frontiers in Medical Technology. 2020. doi: 10.3389/fmedt.2020.610997.
53. Song X, Sui C, Lv M, Jiang C, Hu L, Jiang Y, et al. Dual RNA-seq analysis reveals the interaction between multidrug-resistant Klebsiella pneumoniae and host in a mouse model of pneumonia. BMC Microbiology. 2025. doi: 10.1186/s12866-025-04044-x.

Figures

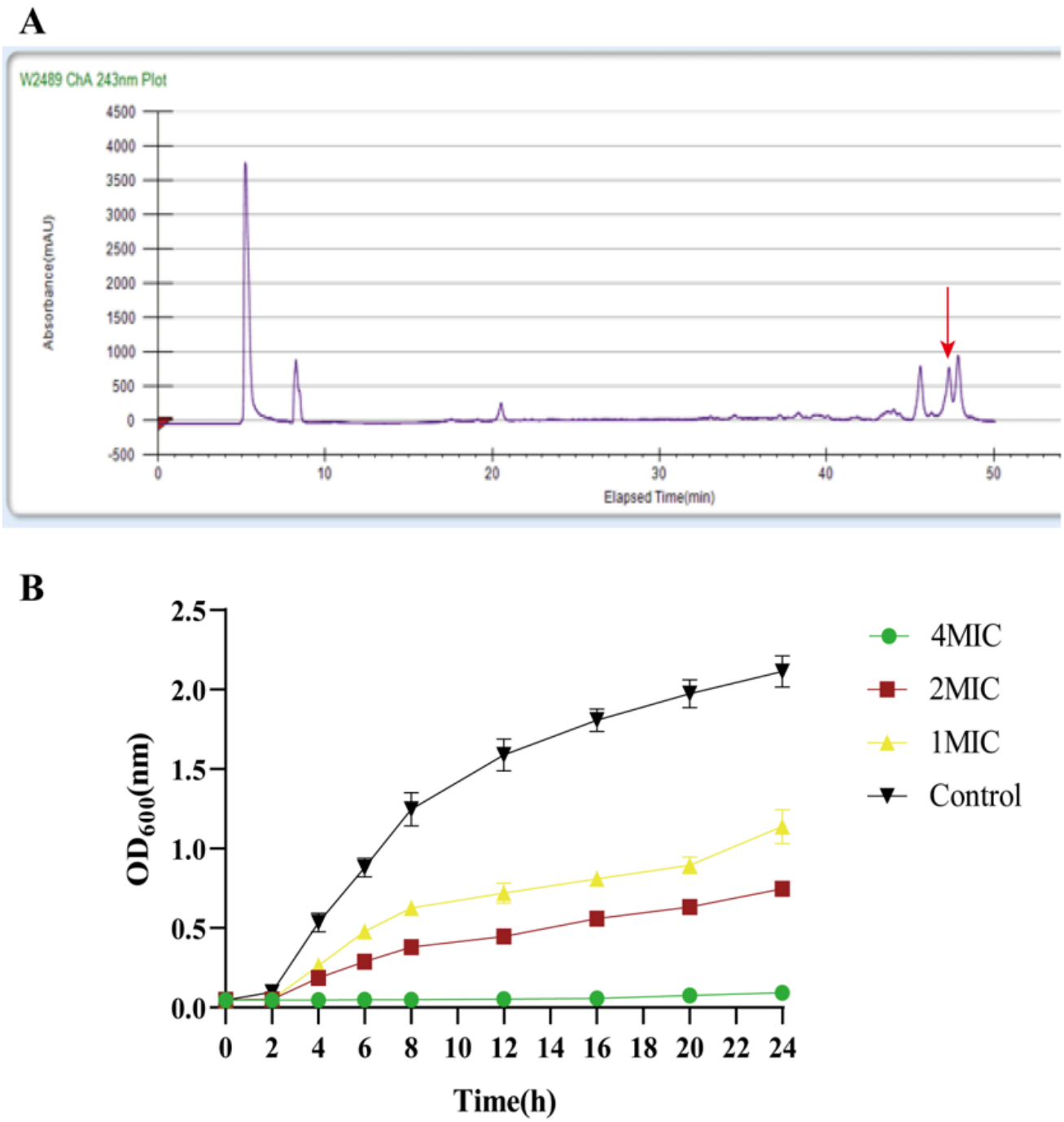


Figure 1

Purification of the bioactive compound from *Bacillus subtilis* Y4 by preparative RP-HPLC and its bactericidal kinetics against MDR-AB. (A) Preparative RP-HPLC elution profile of the purified bioactive compound produced by *Bacillus subtilis* Y4; (B) Bactericidal kinetic curve of MDR-AB treated with oxydifficidin.

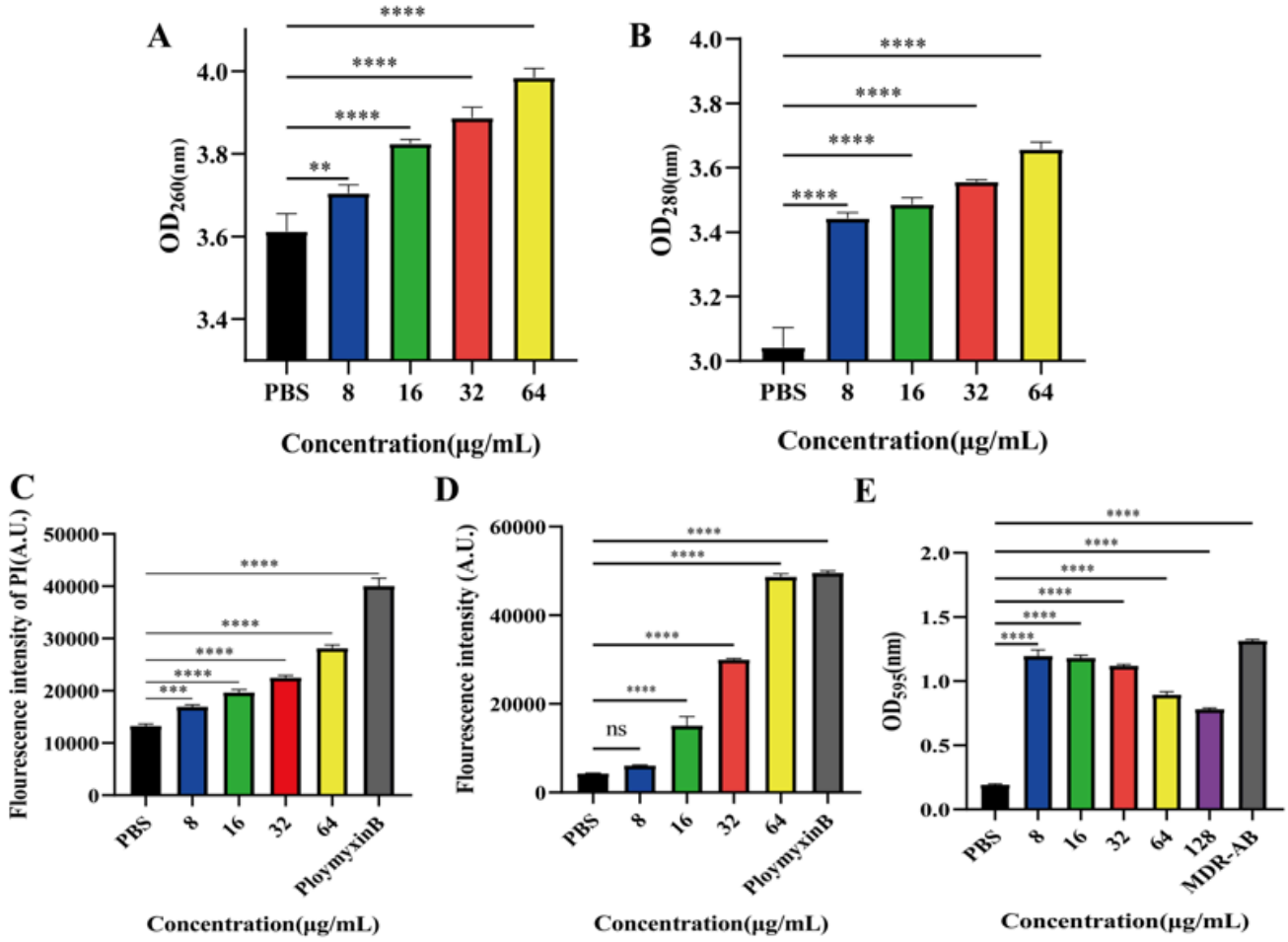


Figure 2

Effects of different concentrations of oxydifficidin on the leakage level of macromolecular substances in MDR-AB. (A) Nucleic acids; (B) Proteins; (C) Effect of oxydifficidin on the cytoplasmic membrane permeability of MDR-AB; (D) Effect of oxydifficidin on the outer membrane permeability of MDR-AB; (E) Effect of oxydifficidin on biofilm formation ability of MDR-AB. Statistical significance is indicated as *p <0.05; **p < 0.01; ***p< 0.001;**** p < 0.0001.

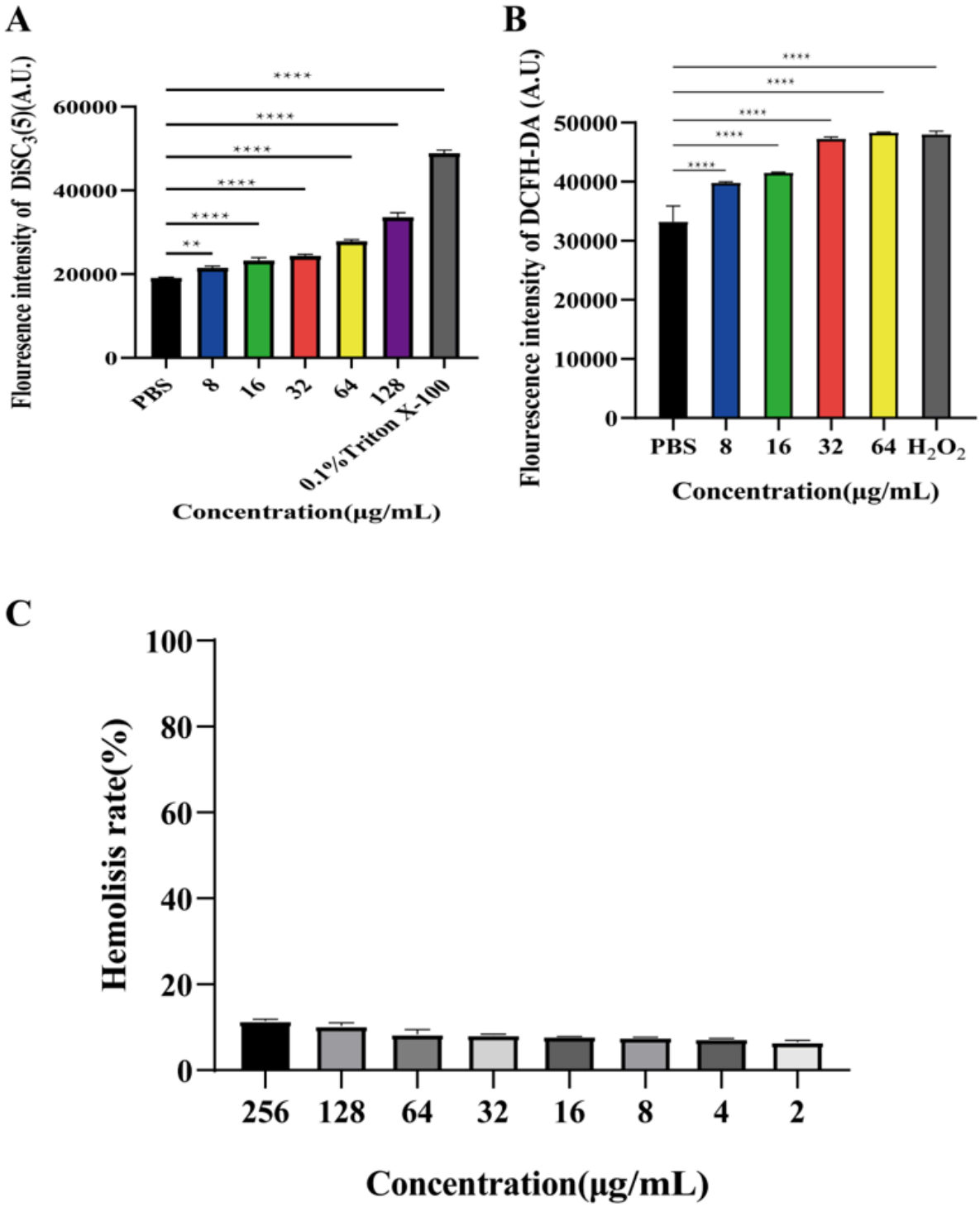


Figure 3

Oxydifficidin exerts antibacterial effects by disrupting membrane potential and inducing oxidative stress in MDR-AB, while exhibiting low hemolytic activity. (A) Membrane potential of MDR-AB cells after treatment with oxydifficidin.(B) Changes in intracellular reactive oxygen species (ROS) accumulation in MDR-AB following oxydifficidin treatment.(C) Hemolytic activity of oxydifficidin against sheep red blood cells. Statistical significance is indicated as *p<0.05; **p < 0.01; ***p < 0.001;**** p < 0.0001.

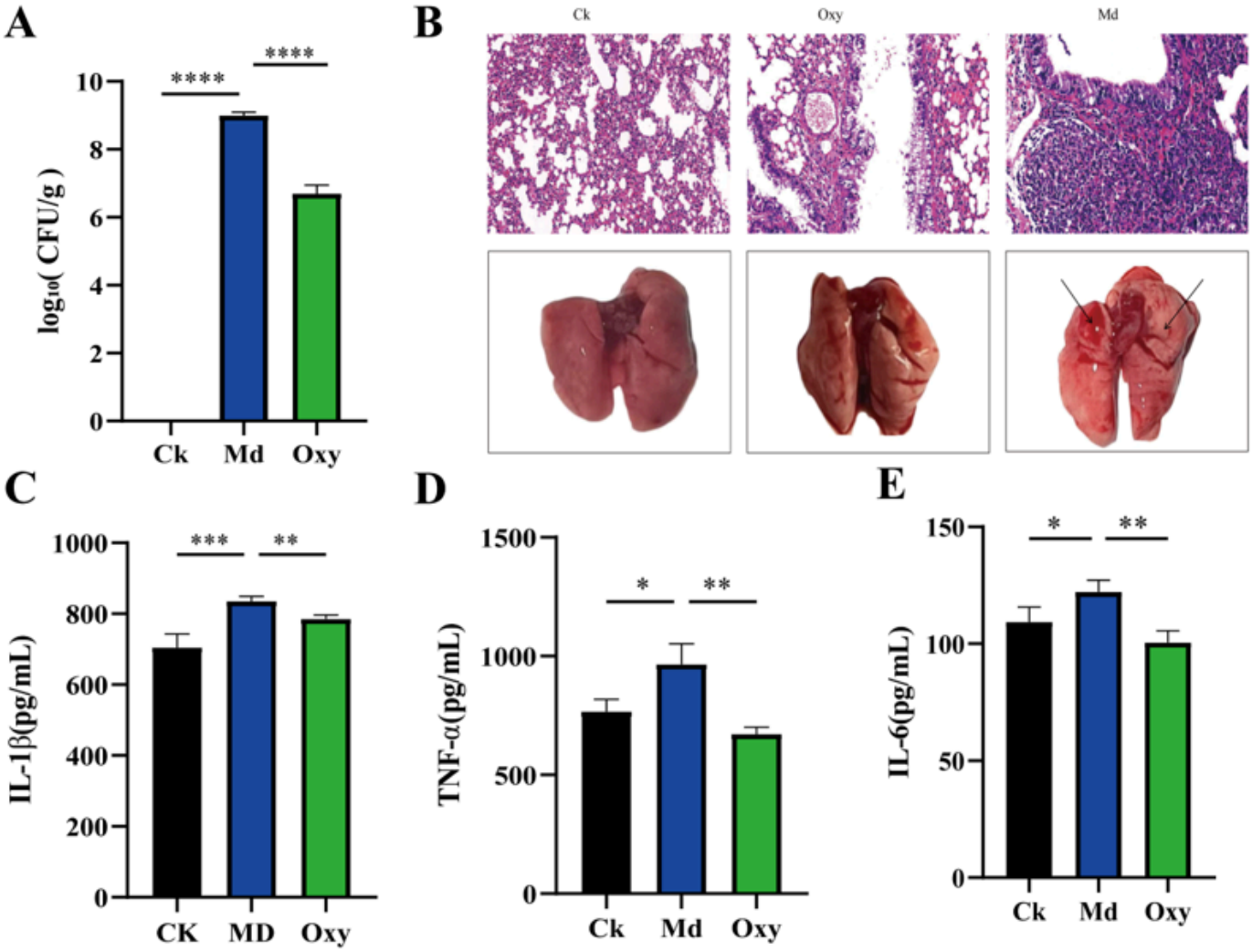


Figure 4

In vivo efficacy of oxydifficidin against MDR-AB.(A) Bacterial loads in the lungs of different groups at 24 h.(B) Representative photographs of lung tissues and H&E-stained lung sections at 24 h; lung necrosis is indicated by blue arrows (scale bar: 100 μm).(C–E) Levels of proinflammatory cytokines IL-1β (C), IL-6 (D), and TNF-α (E) in the lungs at 24 h.Data are presented as mean ± SD (n = 6). Statistical significance is indicated as *p <0.05; **p< 0.01; ***p < 0.001;**** p < 0.0001.

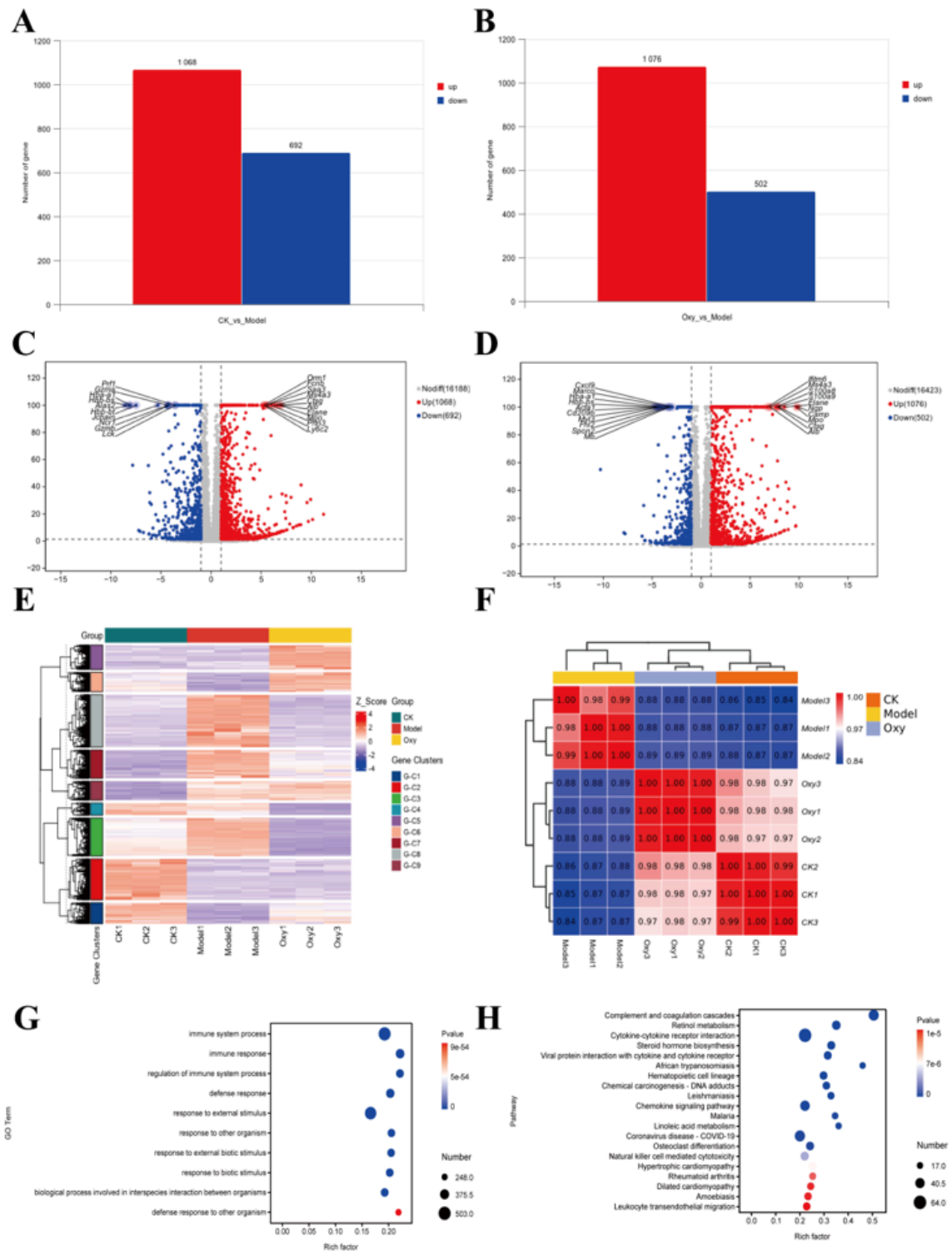


Figure 5

Differentially expressed genes (DEGs) in lung tissues at 24 h after MDR-AB infection.(A) Statistical analysis of DEGs between the Ck and Md groups.(B) Statistical analysis of DEGs between the Oxy and Md groups.(C) Volcano plot of DEGs between the Ck and Md groups.(D) Volcano plot of DEGs between the Oxy and Md groups.(E) Hierarchical clustering heatmap of DEGs.(F) Pearson correlation coefficient heatmap. Functional enrichment analysis of differentially expressed genes (DEGs) in the treatment

group compared with the model group.(G) Gene Ontology (GO) enrichment analysis.(H) Kyoto Encyclopedia of Genes and Genomes (KEGG) pathway enrichment analysis.

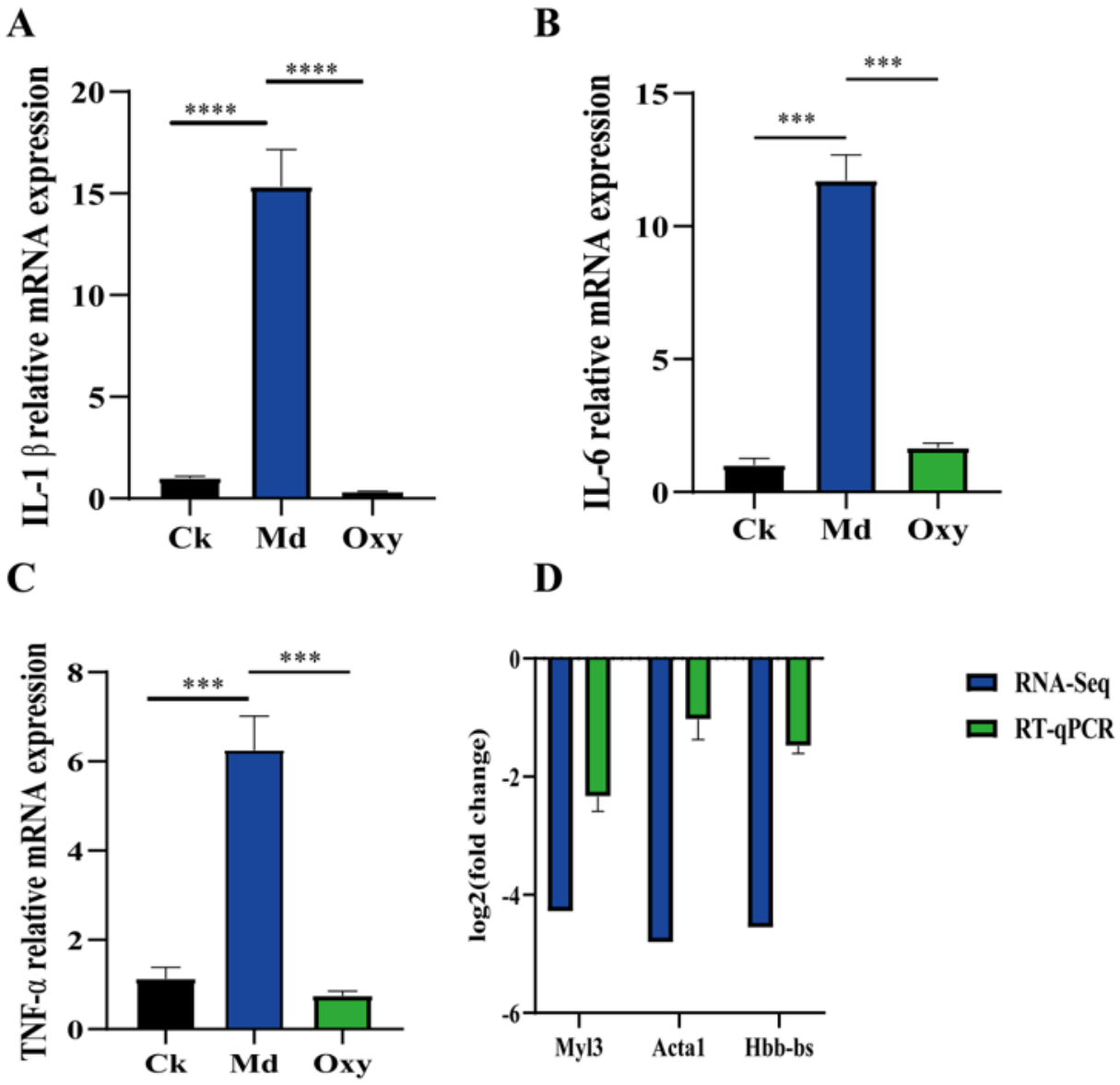


Figure 6

Effects of Oxydifficidin treatment on inflammation-related gene expression. A: IL-1β; B: IL-6; C: TNF-α.The data are the mean ± SD from three replicates of the experiment.(D)Validation results of transcriptome data.Statistical significance is indicated as *p<0.05; **p < 0.01; ***p < 0.001;**** p < 0.0001.

Supplementary Files

This is a list of supplementary files associated with this preprint. Click to download.

- SupplementaryInformation.docx.docx